Instrumented Composite Turbine Blade for Health Monitoring

Kevin E. Robison[1], Steve E. Watkins[1*], *Senior Member SPIE*, James Nicholas[2],
K. Chandrashekhara[2], *and* Joshua L. Rovey[2]
[1]Department of Electrical and Computer Engineering and
[2]Department of Mechanical and Aerospace Engineering
Missouri University of Science & Technology, Rolla, Missouri 65409 USA

ABSTRACT

A health monitoring approach is investigated for hydrokinetic turbine blade applications. In-service monitoring is critical due to the difficult environment for blade inspection and the cost of inspection downtime. Composite blade designs have advantages that include long life in marine environments and great control over mechanical properties. Experimental strain characteristics are determined for static loads and free-vibration loads. These experiments are designed to simulate the dynamic characteristics of hydrokinetic turbine blades. Carbon/epoxy symmetric composite laminates are manufactured using an autoclave process. Four-layer composite beams, eight-layer composite beams, and two-dimensional eight-layer composite blades are instrumented for strain. Experimental results for strain measurements from electrical resistance gages are validated with theoretical characteristics obtained from in-house finite-element analysis for all sample cases. These preliminary tests on the composite samples show good correlation between experimental and finite-element strain results. A health monitoring system is proposed in which damage to a composite structure, e.g. delamination and fiber breakage, causes changes in the strain signature behavior. The system is based on embedded strain sensors and embedded motes in which strain information is demodulated for wireless transmission.

Keywords: Health monitoring, composite blades, strain analysis, smart structures, hydrokinetic power

1. INTRODUCTION

Hydrokinetic systems are promising sources of renewable energy [1]. These systems exploit the kinetic energy from flowing water, tides, and waves. One main category of energy conversion employs a rotating blade and turbine arrangement to couple the fluid flow. These rotating assemblies are of necessity submerged where access and inspection are difficult. In addition, the typical locations are remote. Key aspects for the feasibility of a hydrokinetic system are questions of service life, maintenance needs, and operating costs. In particular, the blades are critical elements and composite blades are good choices for the marine environment (e.g. advantages of ruggedness, light weight, structural flexibility, and corrosion resistance). Blade fatigue due to long-term cyclic loading, blade damage due to impact events, etc. are still concerns. Efficient and economical operation is not possible if blades must be conservatively pulled for physical inspection and if blades fail catastrophically from unattended minor damage. In-situ, remote monitoring is needed. A smart health monitoring approach involves integral sensors and automated instrumentation that monitor structural integrity during operation and that alert service personnel when maintenance, repair, or replacement is needed. Such a system must meet the challenges of an underwater environment and must transmit information from a rotating structure. Little work has been done that specifically meet the remote monitoring needs of a hydrokinetic application.

Smart structures approaches use in-situ sensors and related instrumentation to provide in-service structural monitoring. The performance of composite structures has been frequently studied through parallel theoretical modeling and experimental testing. Load-induced strain is an important parameter that can be readily measured. Damage or degradation to a composite structure, e.g. delamination and fiber breakage, will change the static and dynamic strain

* Author E-mail Addresses: steve.e.watkins@ieee.org, chandra@mst.edu, and roveyj@mst.edu
Contact Author: S. Watkins. 121 EECH, Missouri University of Science and Technology (formerly University of Missouri-Rolla), 301 W. 16th St., Rolla, MO 65409-0040 USA 573-341-6321, Fax 573-341-4532

behavior. A strain signature due to a well-defined load case, such as cyclic operation, is a means of damage assessment. Consequently, a health monitoring system can be based on strain measurement [2-4].

For long-term monitoring of a structure, the choice of sensor becomes important. The sensor must be rugged for field use, must have a long operating life, and must be compatible with the host structure. Smart sensor instrumentation of composite structures has been implemented with piezoelectric and fiber optic approaches, cf. [2-4]. Notably, fiber optic sensors have the capability of being embedded in a composite structure without degrading the host structure. These sensors have advantages of small size, temperature tolerance, high sensitivity, environmental adaptability, etc. [5-9].

In this work, composite blade performance and instrumentation are investigated. Simple four-layer and eight-layer composite beams and three-dimensional, eight-layer blades are considered for free-vibration and static loading. These structures are carbon/epoxy, symmetric composite laminates that were manufactured using an autoclave process. Experimental results for strain measurements from electrical resistance gages are presented in preparation for later embedded sensors. Also, theoretical strain characteristics are presented from in-house, finite-element analysis for all sample cases. Finally, a health monitoring system is proposed that is based on embedded strain sensors and embedded motes in which strain information is demodulated for wireless transmission.

2. STRUCTURES

2.1 Hydrokinetic Turbine Operation

Rotating blade and turbine arrangements are an important form of hydrokinetic technology [1]. System components are the turbine blades, the turbine generator, and power converter. The blades are submerged to capture the kinetic energy of the flowing water current. Blades may be incorporated into horizontal-axis designs or vertical-axis designs. For efficient energy generation, the location must be chosen with regard to strong tides or current flow. For instance, good locations for river applications have natural or argumentation channels to enhance fluid flow. Locations are further constrained by other river uses (e.g. shipping and fishing), seasonal current variations, and environmental impact. For economical operation, key considerations include service life, maintenance needs, and operating costs. The system, and the blades in particular, must operate in possible remote locations and under extreme conditions. The blades are exposed to potentially damaging impacts from debris, ice, etc. Without timely intervention, minor damage may progress to catastrophic failure.

Composite blade structures are well suited for these hydrokinetic applications. With the appropriate constituent materials, composite blades have a long life in marine environments. The structural performance of such blades can be tailored to meet the requirements of hydrokinetic turbines similar to related composite blade designs for wind turbines and aircraft propellers. The compatibility of composite structures with in-situ instrumentation is explored in this work.

2.2 Sample Composite Beams and Blades

The composite samples used for the experiments were fabricated using an autoclave process in the Composite Fabrication Laboratory at Missouri University of Science and Technology. The samples were multilayer carbon/epoxy laminates. Both beam and blade designs were studied. The initial tests were performed on four-layer beams of dimensions 20.32 cm x 2.54 cm x 0.0508 cm (not including the cantilever clamping area). Each laminate of this beam is 0.127 mm thick. A symmetric lay-up sequence of [0/90/90/0] was used with the material ACG(MTM 45-1/HTS563112k).

The next tests were done with eight-layer beams and an eight-layer blade fabricated from identical 0.127-mm laminates. The beam dimensions were 20.32 cm x 2.54 cm x 0.101 cm (not including the clamping area). The blade length was 27.94 cm (not including the clamping area). For both, a symmetric lay-up sequence of [90/90/0/0/0/0/90/90] was used with the material Cytec Cycom 5250/AS4. Figure 1 shows the blade design and Table 1 gives the position, chord length, and thickness of cross-sectional stations measured from the blade root. The material properties are shown in Table 2.

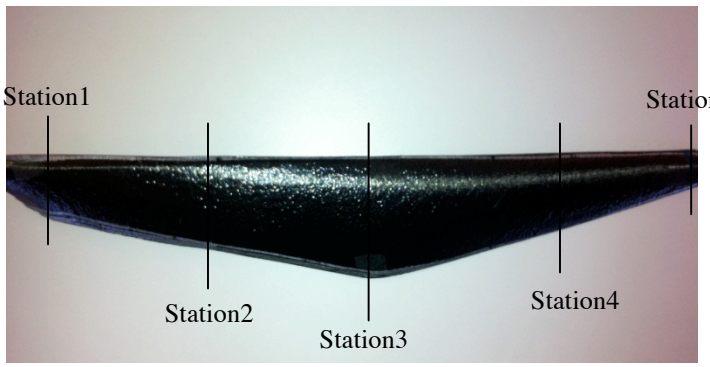

Figure 1. Composite Blade

Table 1. Design of the Composite Blade.

Blade Station	Position from Root (cm)	Chord Length (cm)	Thickness (cm)
1	2.54	3.05	0.101
2	8.89	4.06	0.101
3	15.24	5.46	0.101
4	22.86	3.56	0.101
5	30.48	1.52	0.101

Table 2. Material Properties of the Composite Beams and Blade.

Properties	Four-Layer Beam	Eight-Layer Beam and Blade
Young's Modulus	E_{11} = 138 GPa $E_{22} = E_{33}$ = 8.96 GPa	E_{11} = 143 GPa $E_{22} = E_{33}$ = 10.19 GPa
Poisson's Ratio	$\nu_{12} = \nu_{13} = \nu_{23} = 0.3$	$\nu_{12} = \nu_{13} = \nu_{23} = 0.3$
Shear Modulus	$G_{12} = G_{13}$ = 7.10 GPa G_{23} = 6.8 GPa	$G_{12} = G_{13}$ = 4.01 GPa G_{23} = 3.7 GPa
Density	ρ = 1600 kg/m^3	ρ = 1580 kg/m^3

2.3 Finite-Element Analysis of Composite Structures

A finite-element analysis (FEA) was done using in-house code to predict beam and blade behavior. Cantilever boundary conditions were assumed. The static strain was calculated for a given tip deflection. A free-vibration (dynamic) case was calculated in which the first and second natural frequencies (bending mode) were determined. Figure 2 illustrates the strain distribution from the FE model for top surface of beam under deflection. The beam is supported on the left end. Figure 3 illustrates the strain distribution from the FE model for top surface of blade under deflection. The beam is supported on the left end.

Figure 4 shows the active area of a strain gage on a beam. The FE model calculated the strain at points A, B, and C. Location B is the center of the gage and locations A and C are at the extremes of the gage. An average strain from these three locations was used for comparison to the distributed strain measured by the experimental sensor. The same procedure was used for the blade FE model.

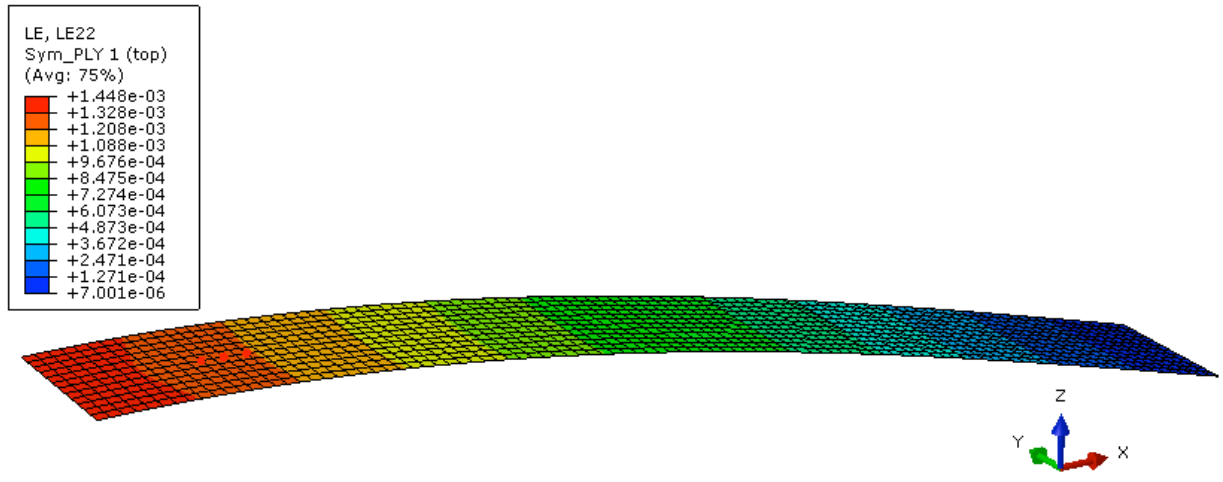

Figure 2. Strain Distribution of the Composite Beam along the Beam Length (x Direction) for Support on the Left End

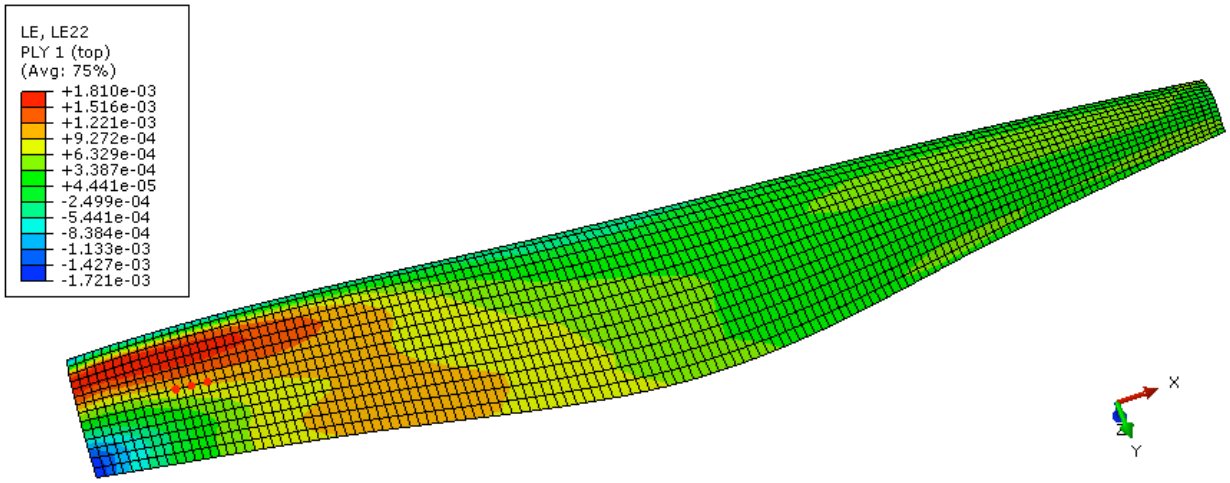

Figure 3. Strain Distribution of the Composite Blade along the Blade Length (x Direction) for Support on the Left End

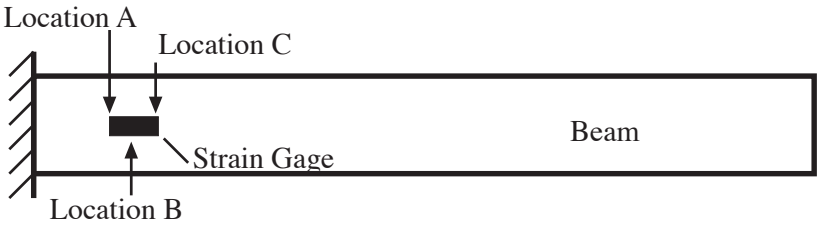

Figure 4. Strain Gage Active Area. The FE Model Calculates Strain at Locations A, B, and C.

3. EXPERIMENTAL PROCEDURE

3.1 Static Strain and Free-Vibration Strain Measurements

The initial test case was for static flexural strain. The procedure was to clamp the beam or blade as a cantilever as shown in Figure 5. In the beam test, the tip was deflected 3.81 cm and the strain measured. In the blade test, the tip was deflected 2.54 cm and the strain measured near the clamped end.

The dynamic test case measured free vibration. Again, the beam or blade was clamped as a cantilever. The tip was deflected 3.81 cm and 2.54 cm for the beam and blade, respectively. After release, the instrumentation captured the strain transient signal. The content of the strain transient was analyzed and the first natural frequency was recorded.

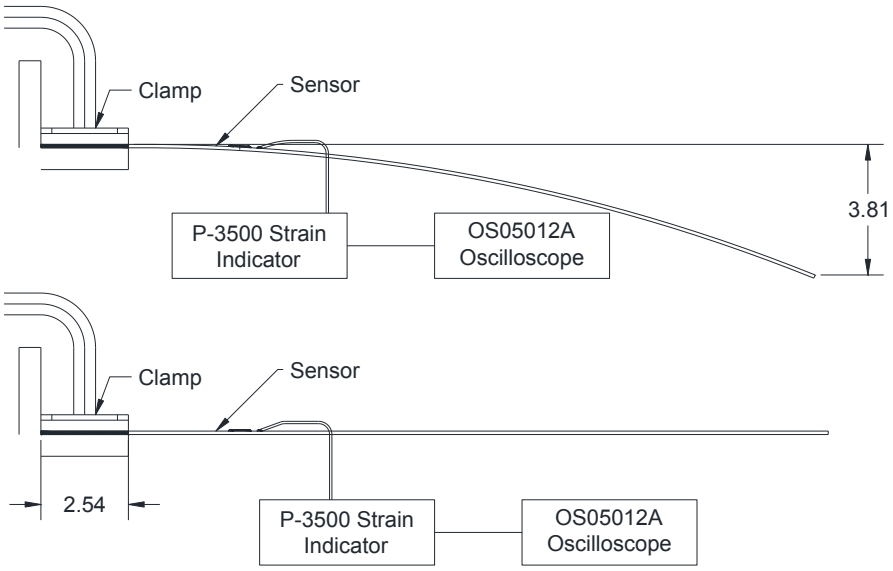

Figure 5. Experimental Setup for Static Strain Test (dimensions in cm)

3.2 Strain Instrumentation

Strain gage sensors were mounted for flexure strain with the gage mid-points located 2.54 cm from the support. Figure 6 and Figure 7 show the sensor layout for the beam and blade, respectively. The shaded regions are for the clamp support. The overall cantilever lengths were 20.32 cm and 27.94 cm, respectively. The gages are centered along the midline of the beams and located 0.64 cm from the leading edge of the blade.

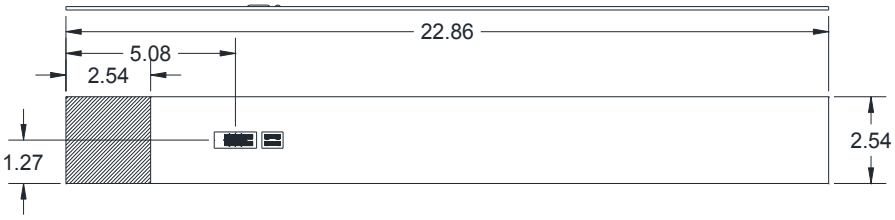

Figure 6. Carbon/Epoxy Composite Beam with Sensor Layout (dimensions in cm)

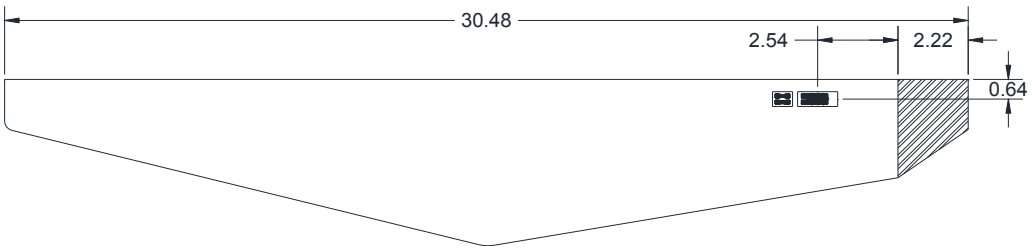

Figure 7. Carbon/Epoxy Composite Blade with Sensor Layout (dimensions in cm)

The strain sensors for the experimental beam and blade tests were 120-Ω electrical resistance gages (Micro-Measurements EA series with 6.35-mm active length). The gages were surface mounted with M-Bond 200 adhesive. The support instrumentation was a Wheatstone bridge strain indicator (Micro-Measurements P-3500) and an oscilloscope.

4. RESULTS AND ANALYSIS

4.1 Beam Tests

The static strain test results for the four-layer and eight layer beams are shown in Table 3. The tip deflection was 3.81 cm. The experimental strain value is compared to the average theoretical strain from the FE model. The average theoretical strain was calculated from the strain at the center of the gage (location B) and the extremes of the gage (location A and C) as shown in Figure 4. The average experimental strain was calculated from multiple measurements on the same beam. The static strains matched within 5.9% and 6.9% for the four-layer and eight-layer beams, respectively. The percent difference was calculated as

$$| (\text{Theoretical Average} - \text{Experimental Average}) / (\text{Theoretical Average}) | \times 100.$$

Table 3. Static Strain Results for the Composite Beams.

Beam Type	Theoretical Strain at A (microstrain)	Theoretical Strain at B (microstrain)	Theoretical Strain at C (microstrain)	Theoretical Average (microstrain)	Experimental Average (microstrain)	Percent Difference
Four-Layer Beam	628.49	615.74	596.91	613.71	650 $\pm$ 5	5.9%
Eight-Layer Beam	1274.39	1248.60	1209.55	1244.18	1230 $\pm$ 5	6.9%

The free-vibration test results for the eight-layer beam are shown in Table 4 and Figure 8. The tip deflection was 3.81 cm. The first and second natural frequencies from the FEA model are shown. Both frequencies refer to bending modes. The experimental result for the first natural frequency is shown; the second natural frequency was not recorded due to instrument limitations. The experimental frequency closely matched the theoretical prediction.

Table 4. Free-Vibration Results for the Eight-Layer Composite Beam.

	Theoretical Natural Frequencies (Hz)		Experimental Natural Frequency (Hz)
Eight-Layer Beam	1st 16.40 Hz 2nd 102.7 Hz		1st 16.1 Hz

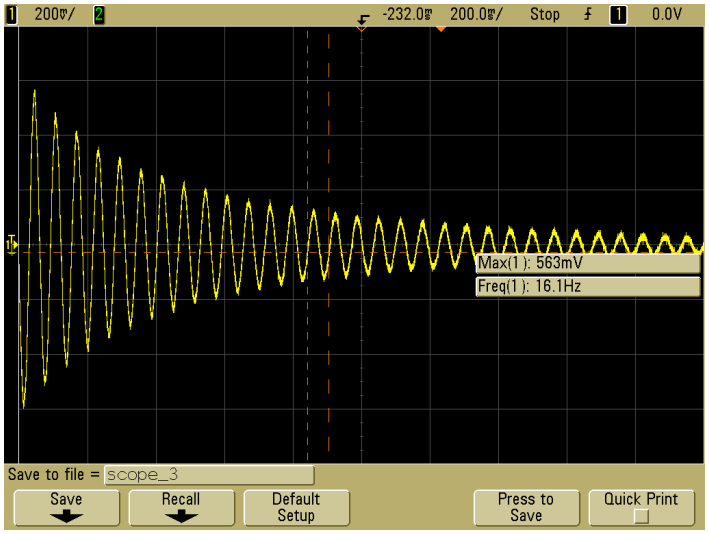

Figure 8. Free-Vibration Strain Transient for the Eight-Layer Composite Beam

4.2 Blade Tests

The static strain test results for the blade are shown in Table 5. The tip deflection was 2.54 cm. The experimental strain value is compared to the theoretical strain, i.e. the average strain of the ABC locations, from the FE model. The percent difference is calculated as for the beam tests. The static strains differ by 16.4%. Note that the theoretical strain varies significantly over the gage active area.

The free-vibration test results for the blade are shown in Table 6. The strain transient is similar to that in Figure 8. The first and second natural frequencies from the FEA model are shown. Both frequencies refer to bending modes. Here the first natural frequency differs by more than a factor of two. The cause of this difference is not clear and will be explored in future tests.

Table 5. Static Strain Results for the Composite Blade.

Type	Theoretical Strain at A (microstrain)	Theoretical Strain at B (microstrain)	Theoretical Strain at C (microstrain)	Theoretical Average (microstrain)	Experimental Average (microstrain)	Percent Difference
Blade	704.51	813.17	1111.04	876.24	1020 $\pm$ 5	16.4%

Table 6. Free-Vibration Results for the Composite Blade.

	Theoretical Natural Frequencies (Hz)		Experimental Natural Frequency (Hz)
Blade	1st 38.63 Hz 2nd 76.04 Hz		1st 15.6 Hz

5. SUMMARY AND PROPOSED HEALTH MONITORING SYSTEM

Strain characteristics of composite beams and blades were investigated. A composite blade was successfully fabricated and instrumented. Samples were experimentally and theoretically analyzed for static and dynamic strain characteristics. The strain results from experiment behavior and the theoretical analysis generally matched. The test cases measured static flexural strain and the free-vibration dynamic response. All samples were undamaged, but these results will be compared to that of otherwise-identical damaged blades in future work. The application area is hydrokinetic turbine technology. This work is a preliminary step to understanding the strain behavior of composite blades for rotating turbine applications. The immediate goal is to understand the strain signature for normal cyclic operation and for impact events. Changes in this signature need to be linked to structural health. The long-term goal is to assess the feasibility of a health monitoring approach.

The proposed health monitoring system is illustrated in Figure 9(a). This arrangement avoids the difficulty of having a physical connection, e.g. electrical wire or optical fiber, from the rotating blade to the health monitoring station. The submerged turbine blade is instrumented with an embedded fiber optic strain sensor and the support electronics module is housed in the blade hub. The signal is passed to an embedded ultrasonic transducer for transmission to a receiver placed in a convenient location. Depending on the degree of intelligence in the support module, the strain signal may be simply demodulated and transmitted for further processing or may be processed and the healthy/unhealthy indication transmitted. The first approach requires more information in the transmission and less complex processing while the second approach requires little transmission capacity and intelligent processing.

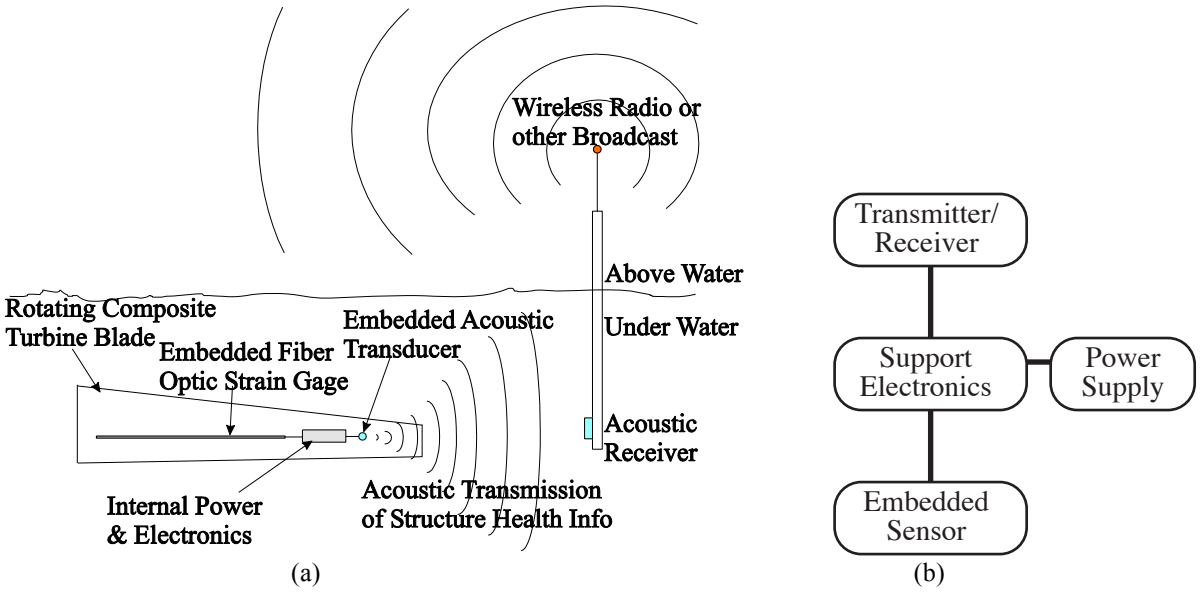

Figure 9. (a) Proposed Smart Health Monitoring System and (b) Major Subsystems

A block diagram of this health monitoring system is shown in Figure 9(b). The three major subsystems are the ultrasonic transmitter/receiver, the support electronics, and the embedded sensor. Preliminary work on the ultrasonic transmission is described in an associated work [10]. A good choice for the strain sensor is a fiber optic strain sensor. Either Bragg or Fabry-Perot interferometric sensors are possible [3-9]. Such sensors are suitable to be embedded in a composite structure and have the ruggedness to survive for long-term operation, cf. [4]. Work is needed on demodulating and processing the optical signal for the specific cyclic loading of the blade. Neural network approaches similar to those discussed for periodic and damped vibration excitation are candidates for this application [11,12]. The electronic hardware and the needed power supply must be embedded as well and may be based on advances in sensor motes and nodes [13,14].

Further development of this health monitoring approach for turbine blades requires a full characterization of blade behavior and advances in sensing, instrumentation, and data acquisition. The composite blade behavior, for undamaged and damaged cases, must be experimental and theoretical verified for dynamic loading that is representative of typical hydrokinetic operation, e.g. operation in water and under cyclic loading. The strain characterization will give a tool for evaluating blade design and will give insight toward the needed processing for the strain signal processing. For instance, what are the features in a strain signature that are closely linked to common damage and what intelligent processing is needed to highlight these features? Fiber optic sensors need to be incorporated in turbine blades and the blade performance needs to be characterized for expected damage mechanisms. Embedded instrumentation must be tailored for demodulation of the sensor signals and must be incorporated into the blade hub. The embedded instrumentation must be integrated with the ultrasonic transmitter.

ACKNOWLEDGEMENTS

The authors wish to thank the Office of Naval Research (grant N00014-10-0923) and the Department of Energy (grant DE-EE0004569) for supporting this work.

REFERENCES

[1] Khan, M. J., Bhuyan, G., Iqbal, M. T., and Quaicoe, J. E., "Hydrokinetic energy conversion systems and assessment of horizontal and vertical axis turbines for river and tidal applications: A technology status review," Applied Energy 86, 1823-1835 (2009).

[2] Okafor, A. C., Chandrashekhara K., and Jiang Y. P., "Delamination prediction in composite beams with built-in piezoelectric devices using modal analysis and neural network," Smart Materials and Structures 5(3), 338-347 (1996).

[3] Watkins, S. E., Sanders, G. W., Akhavan, F., and Chandrashekhara, K., "Modal Analysis using Fiber Optic Sensors and Neural Networks for Prediction of Composite Beam Delamination," Smart Materials and Structures 11(4), 489-495 (2002).

[4] Zetterlind III, V. E., Watkins, S. E., and Spoltman, M. W., "Feasibility Study of Embedded Fiber-Optic Strain Sensing for Composite Propeller Blades," Proc. SPIE 4332, 143-152 (2001).

[5] Han, L., Voloshin, A., and Coulter, J., "Application of the integrating fiber optic sensor for vibration monitoring," Smart Materials and Structures 4(2), 100-105 (1995).

[6] Measures, R. M., "Advances toward fiber optic based smart structures," Optical Engineering 31(1), 34-47 (1992).

[7] Reid, M.B. and Ozcan, M., "Temperature dependence of fiber optic Bragg grating at low temperature," Optical Engineering 37(1), 237-240 (1998).

[8] Zhao, W., Wang, J., Wang, A. and Claus, R. O., "Geometric analysis of optical fiber EFPI sensor performance," Smart Materials and Structures 7(6), 907-910 (1998).

[9] Davis, M. A., Kersey, A. D., Sirkis, J. and Friebele, E. J., "Fiberoptic Bragg grating array for shape and vibration mode sensing," Smart Materials and Structures 5(6), 759-65 (1996).

[10] Heckman, A. J., Rovey, J. L., Chandrashekhara, K., Watkins, S. E., Mishra, R., and Stutts, D., "Ultrasonic underwater transmission of composite turbine blade structural health," Proc. SPIE 8343, (2012).

[11] Mitchell, K., Ebel, W., and Watkins, S. E., "Low-power hardware implementation of artificial neural network strain detection for extrinsic Fabry-Perot interferometric sensors under sinusoidal excitation," Optical Engineering 48(11), 114402 (2009).

[12] Dua, R., and Watkins, S. E., "Near real-time analysis of extrinsic Fabry-Perot interferometric sensors under damped vibration using artificial neural networks," Proc. SPIE 7292, (2009).

[13] Fonda, J. W., Watkins, S. E., Sarangapani, J., and Zawodniok, M., "Embeddable sensor mote for structural monitoring," Proc. SPIE 6932, (2008).

[14] Mitchell, K., Watkins, S. E., Fonda, J. W., and Sarangapani, J., "Embeddable modular hardware for multi-functional sensor networks," Smart Materials and Structures 16(5), N27-N34 (2007).